Health Indices Based on Morphology and Complexity Measures of Vibration Signals for Machine Condition Monitoring and Prognostics

B. Samanta† and C. Nataraj

Department of Mechanical Engineering, Villanova University, Villanova, PA 19085, USA
biswanath.samanta@villanova.edu
c.nataraj@villanova.edu

ABSTRACT

The paper presents health indices (HI) for monitoring and prognostics of machine condition. HI are developed using morphology and entropy based complexity measures of machine vibration signals. The indices are compared with a recently introduced energy based feature and the commonly used statistical measure of signal kurtosis. The procedure of extracting HI is illustrated first using the simulated response of a simple gear model with tooth crack. Next the HI extraction process is applied to the experimental vibration data of a helicopter drivetrain gearbox with a seeded tooth fault. The effectiveness of the extracted HI is compared for gear condition monitoring and prognostics.*

1 INTRODUCTION

Prognostics and health management (PHM) is gaining importance as a requirement for the reliability of safety critical systems used in aerospace, military and commercial applications that mandate continuous uptime. PHM is critical to condition based maintenance (CBM) and reliability assurance of engineering systems. The assessment of machine condition utilizes various temporal patterns including oil-debris analysis, temperature profile, acoustic and vibration signals. Due to ease of measurement and analysis, vibration based monitoring and prognostic approach is quite common in CBM of machines (Heng et al., 2009; Vachtsevanos et al., 2006; Jardine et al., 2006; Hardman et al., 1999).

CBM involves three principal steps, namely, data acquisition, signal processing, and maintenance decision-making based on diagnostics and prognostics. The signal processing step involves analysis of the acquired vibration data to identify a suitable health index (HI) characterizing the machine condition, both in type and level of faults. The remaining useful life (RUL) can be estimated for a predefined threshold from the trend of HI. The HI include time domain features (Honchmann and Bechhoefer, 2003; Samanta, 2004; Choi and Li, 2006; He and Bechhoefer, 2008; Samanta and Nataraj, 2009a), frequency spectrum (Zakrajsek et al., 1995), wavelet amplitude pattern of residual signal (Wang et al., 2004; Samanta and Nataraj, 2008a), signal energy (Al-Balushi and Samanta, 2002; Samanta and Nataraj, 2009b), and signal complexity measures (Yu et al., 2006; Yan and Gao, 2007; Janjarasjitt et al., 2008), among others.

Several measures like approximate entropy (ApEn), sample entropy (SampEn), and multiscale entropy (MSE) have been proposed as indicators of complexity (or lack of regularity) of time series signals in biomedical domain (Pincus, 1991; Richman and Moorman, 2000; Costa et al., 2005). These information entropy based features are used for short and noisy physiological signals as alternatives to other nonlinear system measures like Lyapunov exponent and correlation dimension (Henry et al., 2002). SampEn has been shown to have better accuracy than ApEn over a wide range of conditions (Richman and Moorman 2000). The MSE introduced by Costa et al. (2005) measures complexity of the time series by computing SampEn over multiple scales. The scale factor is one for the original signal. For each scale factor, a new time series is constructed by dividing the original time series into non-overlapping windows of length equal to the scale, with each window being replaced by its average.

† Corresponding author

Some of these signal complexity measures, namely ApEn and permutation entropy, have been used for machine condition monitoring (Yu et al., 2006; Yan and Gao, 2007; Janjarasjitt et al., 2008). However, there is a need to study the effectiveness of these complexity measures as potential HI in comparison with other measures for condition monitoring and prognostics of machines.

Mathematical morphology (MM) was introduced to analyze shape-size complexity of images through basic morphological operations of erosion (contraction), dilation (expansion), opening (erosion followed by dilation) and closing (dilation followed by erosion) using a simple structuring element (SE) (Maragos and Schafer, 1987; Maragos, 1989a; 1989b). Though the initial applications of MM were mainly in the field of image processing and analysis, there have been growing interests in other domains including biomedical signal processing (Sun et al., 2003; Sun et al., 2005; Xu et al., 2007). In recent years, morphological signal processing (MSP) has been used on vibration signals for detection and diagnosis of machine conditions (Nikolaou and Antoniadis, 2003; Zhang et al., 2008; Wang et al., 2009). In a recent work (Samanta and Nataraj, 2008b), the authors used MSP to extract multiscale pattern spectrum (PS) (Maragos, 1989b) and proposed a novel entropy based feature from PS as the HI for monitoring and prognostics of machinery condition.

The present work uses the information entropy based complexity measure SampEn and compares it with the PS entropy (PSEn) for development of suitable HI. These indicators are also compared with energy based feature called energy index (Al-Balushi and Samanta, 2002; Samanta and Nataraj, 2009b) and signal kurtosis. In this work, each HI has been developed using the evolving average of the feature instead of its instantaneous value, similar to (Samanta and Nataraj, 2008b; 2009b). The procedure of feature extraction has been illustrated using the simulated time response of a simple gear model with a tooth crack (Smith, 2003; Honchmann and Bechhoefer, 2003). The effect of tooth crack has been modeled as a reduction in tooth stiffness during its engagement. Next, the process of HI development has been applied to the vibration dataset of a helicopter drivetrain gearbox with a seeded tooth fault (Hardman et al., 1999).The effectiveness of these HI has been compared for both datasets.

The rest of the paper is organized as follows. Section 2 briefly presents the background information on MSP and the formulation of the PS entropy based HI. Section 3 gives a brief discussion on the complexity measure SampEn. In Section 4, energy based feature EI is briefly discussed. Section 5 presents the evolutionary average of the HI. Section 6 describes a simple model for simulating the dynamics of a spur gear pair with a crack developing in one of the teeth. In section 7, results on HI are presented for vibration data of the simulated gear response and the helicopter gearbox test data. The salient features of the present work are summarized in section 8.

2 MORPHOLOGICAL SIGNAL PROCESSING

In this section, analysis of time domain vibration signals using MSP is briefly discussed for completeness. For details, readers are referred to (Maragos and Schafer, 1987; Maragos, 1989a; 1989b; Samanta and Nataraj, 2008b).

2.1 Basic Morphological Operations

The basic idea of MSP is to modify and extract the geometrical features of a signal by its morphological convolution with another object of simpler shape and size, termed as structuring element (SE). The selection of SE, in terms of shape and size (scale), is an important issue in MSP. The basic morphological operations are defined for a one-dimensional sampled function f(i) with a discrete-valued SE, g(j), ($i \in I$, $j \in J$, $J<I$) as follows:

$$\text{Erosion:} \quad (f \ominus g)(i) = \min(f(i+j) - g(j)), \tag{1}$$

$$\text{Dilation:} \quad (f \oplus g)(i) = \max(f(i-j) + g(j)), \tag{2}$$

$$\text{Opening:} \quad (f \circ g)(i) = ((f \ominus g) \oplus g)(i), \tag{3}$$

$$\text{Closing:} \quad (f \bullet g)(i) = ((f \oplus g) \ominus g)(i). \tag{4}$$

where $\ominus$, $\oplus$, $\circ$ and $\bullet$ denote morphological operators for erosion, dilation, opening and closing respectively. For a sampled signal with a small, flat SE, the erosion of the signal reduces the peaks and enlarges the minima. Similarly, the dilation of the signal increases the valleys and enlarges the maxima. The opening operation smoothens the time signal from below cutting down the peaks and the closing operation smoothens the signal from top filling up the valleys. Thus closing and opening operations can be used to detect peaks and valleys respectively in a signal. The peaks (valleys) of the function can be obtained subtracting opening (closing) from the function. This is quite useful in analyzing signals of impulsive nature, especially in the presence of machinery faults and background noise. The scale of SE should be larger than the widths of the peaks and the valleys for proper detection and or elimination of the peaks and valleys (Nikolaou and Antoniadis, 2003).

2.2 Multiscale Morphology Analysis and Pattern Spectrum

Most of the traditional MM used single-scale analysis with a SE of fixed scale selected *a priori* based on the

nature of the signal. Quite often in single-scale applications, it is not possible to have the prior knowledge for selecting the scale of a SE. The *a priori* selection of scale in traditional MM is overcome with the introduction of multiscale morphological filters (Maragos, 1989b). In the multiscale approach, SE of scales (n=0,1,2,..., N) are used for morphological analysis. For a discrete-valued function g(j), $j \in J$, used as the basic SE, the function pattern can be defined as follows:

$$\begin{cases} ng = g \oplus g \oplus g ... \oplus g \ \text{(n times)}, \\ 0g = \{0\}. \end{cases} \quad (5)$$

For a nonnegative sampled signal, f(i), $i \in I$ and a SE, g, PS is defined as follows:

$$PS(f,g,+n) = S[f \circ ng - f \circ (n+1)g], \quad 0 \le n \le N, \quad (6)$$

$$PS(f,g,-n) = S[f \bullet ng - f \bullet (n-1)g], \quad 1 \le n \le K. \quad (7)$$

Where $S(f) = \sum_i f(i)$, *N* is the maximum size of n such that $f \Theta ng$ is not all $-\infty$, f has sufficient dc-bias such that $f \circ g \ge 0$, $\forall n \le N$ and *K* is the minimum size of *n*.

The PS contains useful qualitative information about the signal (f) shape and size relative to the SE (*g*). The degree of shape content of g in f is given as normalized PS:

$$q(n) = PS(f,g,n)/S(f). \quad (8)$$

It is worth mentioning that MSP has some apparent similarities with wavelet transform (WT). For example, SE is similar to mother wavelet, and both MSP and WT are applicable for processing non-stationary signals. The distinguishing feature between these techniques is that MSP is capable of handling nonlinearity of signals whereas WT is limited to linear signals. In some recent applications, both MSP and WT have been used combining their advantages (Jia et al., 2006). In the present paper, MSP is preferred to WT because of the capability of MSP in handling nonlinear signals commonly encountered in rotating machines.

2.3 Pattern Spectrum Entropy

The quantitative measure of shape-size complexity of a signal relative to a SE pattern is obtained as an average roughness from its PS using the concepts of information theory (Maragos, 1989b):

$$H(f/g) = -\sum_{n=0}^{N} q(n) \log q(n). \quad (9)$$

H(f/g) is termed as PS entropy and its normalized form is defined as:

$$H_r(f/g) = H(f,g,n)/\log(N+1). \quad (10)$$

There are two versions of normalized PS entropy, H_{rO} and H_{rC}, corresponding to PS with opening PS(f,g,+n) and closing PS(f,g,-n), respectively.

3 SAMPLE ENTROPY

Among different complexity measures, sample entropy (SampEn) is considered in this work. This section gives a brief discussion on SampEn. For details, readers are referred to (Richman and Moorman, 2000). SampEn is defined as the negative logarithm of the conditional probability that two sequences that are similar for m points (dimension m), remain similar at the next point (m+1), within a tolerance r, Eq. (11). The probability density function is estimated using Eq. (12), where Λ represents Heaviside function and L is the length of the time series.

$$SampEn(m,r,L) = -\ln\left(\frac{A^{m+1}(r)}{A^{m}(r)}\right) \quad (11)$$

$$A^{m}(r) = \frac{2}{L(L-1)} \sum_{i=1}^{L} \sum_{j=1}^{L} \Lambda\left(r - \left\| x_i^m - x_j^m \right\|\right) \quad (12)$$

SampEn is widely used for nonlinear discrimination between datasets based on the lack of regularity or complexity of their underlying dynamics. A time series with higher complexity (or less regularity) will have a higher value of SampEn than a more regular one (with higher degree of predictability).

4 ENERGY INDEX (EI)

In this Section, a brief review is presented on the energy based feature proposed in previous research (Al-Balushi and Samanta, 2002; Samanta and Nataraj, 2009b) for condition monitoring of machines. EI is defined as square of the ratio between root mean square (RMS) value for a segment of the signal and the overall RMS value of the entire signal. For a uniform consistent signal, the value of EI is 1.0 for all segments. However, for a segment which has relatively higher activities, either in the form of high amplitude levels or additional high frequency energy components, the value of EI will be higher than 1.0, while it will be less than 1.0 for other segments with relatively lower level of activities. The higher the value of EI, the greater is the energy concentration for that specific segment which needs to be monitored.

For a gearbox signal, the segment energy corresponds to the duration of engagement of each gear tooth, and the total energy corresponds to one complete revolution of the gear wheel. In this development, it is

assumed that the number of teeth in the gear under investigation is known *a priori*. It is also assumed that the gear speed is constant over a complete revolution (cycle) even though the speed may vary between cycles. The proposed feature (*EI*) will be applicable even if the meshing periods vary between the cycles. Under the assumption of constant gear speed over a cycle, the meshing period of a tooth is constant and the independent variable, time of sampling over a cycle, may be replaced by the angular position of the gear. The time to angle transformation, in presence of variation in instantaneous gear speed over a cycle, can be taken care of by interpolating the gearbox signal and re-sampling it at the intervals matching exactly with the required angular increments. In this approach, both the gearbox signal and the gear shaft rotational speed can be sampled at fixed rates.

In terms of signal samples, *EI* for individual gear tooth *i* and time index (cycle number) *k*, *EI(i,k)*, can be obtained as follows:

$$\mathrm{EI}(\mathrm{i},\mathrm{k}) = \left\{ \frac{\frac{1}{N_T} \sum_{j=(i-1)N_T+1}^{iN_T} (x(j,k))^2}{\frac{1}{L} \sum_{j=1}^{L} (x(j,k))^2} \right\} \tag{13}$$

where indices *i*, *j*, and *k* represent the current number of gear tooth, sample (within a cycle) and time index (cycle number) respectively, $i\ (1 \le i \le P), j\ (1 \le j \le L)$ and $k\ (1 \le k \le M)$. The parameters *P*, *N* and *M* represent the total number of teeth, samples for one revolution of the gear, and cycles respectively. N_T represents number of samples corresponding to one gear tooth. *x(j,k)* represents the value of sample *j* at time index *k* and is considered to be a random variable. It should be noted that the first point of the time series *x(1,k)* corresponds to the beginning of the first gear tooth for each cycle so that each N_T samples correspond to a single tooth without any overlap. In Eq. (13), the numerator is the expected value of the mean square (*MS*) of samples within the shifting window that frames individual tooth as it travels from the first to the last. The denominator of the equation represents the expected value of the *MS* of the whole signal and needs to be computed only once for a cycle.

5 EVOLUTIONARY AVERAGE HI

In an earlier work (Al-Balushi and Samanta, 2002) several forms of EI, namely, cumulative (cEI) and evolutionary average (aEI) were proposed and their relative effectiveness in diagnosing the machine state were demonstrated. The main advantage of using cumulative value, *cEI*, over the current value of *EI* is that the recurring events show up prominently in the plot of *cEI* as the corresponding energy contributions add up. The spurious events become insignificant in the plot of *cEI* as the contributions are not consistent although these may have high values of *EI* at certain points of time. The *EI* values between any two successive cycles can be clearly seen from the plot of *cEI*. These features are useful in identifying the localized faults. The cumulative value of a feature (*EI*) gives an indication about the accumulation of the value over the entire period of investigation. The concept of evolutionary average of EI has been extended to other features (HI) to represent the variation over the period for any tooth *i* at time (cycle) index *k(>0)*, as follows:

$$\mathrm{aHI}(\mathrm{i},\mathrm{k}) = \begin{cases} 0, & \mathrm{k} = 0 \\ \frac{1}{\mathrm{k}} \sum_{\mathrm{l}=1}^{\mathrm{k}} \mathrm{HI}(\mathrm{i},\mathrm{l}), & \mathrm{k} > 0 \end{cases} \tag{14}$$

In the present work, evolutionary average of each HI has been used as the monitoring index for gear condition.

6 GEAR CRACK MODEL

The dynamic model for simulating vibration of a gear pair in mesh can be represented in form of an equivalent single degree of freedom system as follows (Smith 2003; Hochmann and Bechhoefer, 2003):

$$I_e\ddot{x}(t) + c\dot{x}(t) + s\big(\theta(t)\big)x(t) = I_e F_e + s\big(\theta(t)\big)e(t) \tag{15}$$

where I_e is the equivalent mass of the gear pair, c is the system viscous damping coefficient, *s* is the tooth stiffness, *x*(*t*) is the time varying gear vibration, F_e is the equivalent force due to the input and output torques on the gear pair, $\theta(t)$ is the gear rotation and *e*(*t*) is the gear transmission error. The expressions for the equivalent mass and the external force are given as follows:

$$\mathrm{I_e} = \frac{\mathrm{I_p I_g}}{\mathrm{I_p r_g^2 + I_g r_p^2}} \tag{16}$$

$$\mathrm{F_e} = \frac{\mathrm{r_p}}{\mathrm{I_p}} \mathrm{T_{in}} + \frac{\mathrm{r_g}}{\mathrm{Ig}} \mathrm{T_{out}} \tag{17}$$

where I_p, I_g are the rotary inertia of the pinion and the gear, r_p and r_g are the corresponding pitch radii, and T_{in} and T_{out} are the input and the output torques respectively. The gear mesh stiffness depends on the gear rotation angle. The effect of crack in a tooth is modeled as a step reduction in stiffness during the period of engagement of the tooth as follows:

$$\mathrm{s}(\theta(\mathrm{t})) = \begin{cases} \alpha \mathrm{s}, & \theta_\mathrm{i}(\mathrm{t}) < \theta(\mathrm{t}) \le \theta_{\mathrm{i+1}}(\mathrm{t}) \\ \mathrm{s}, & \text{otherwise} \end{cases} \tag{18}$$

where i represents the number of the tooth under consideration and $\theta_i(t) < \theta(t) \leq \theta_{i+1}(t)$ represents the range of the gear angle when the ith tooth is engaged. The factor α is a positive number, $0<\alpha\leq 1$, a value of $\alpha=1$ represents a tooth with no crack and a value of $\alpha=0$ means the total loss of the tooth.

7 RESULTS AND DISCUSSIONS

This section presents the results of feature extraction using the simulated vibration data of a gear pair with a tooth crack and the experimental dataset of a helicopter drive train gearbox with a seeded tooth fault.

7.1 HI for Simulated Data of Gear Tooth Crack

The procedure is illustrated through the simulated dynamic response of a spur gear pair using Eq. (15). The effect of tooth crack is studied considering the tooth mesh stiffness to be constant (s) throughout the gear rotation except when the tooth is engaged as discussed in Eq. (18). The level of crack is simulated through a lower value of factor α. The parameters, similar to those used by Hochmann and Bechhoefer (2003) are given in Table 1. A nominal speed of 800 rpm is used with 20 teeth for each gear. A normal distribution with an assumed mean and variance has been used as the static transmission error, $e(t)$. The weakening effect of the gear tooth crack has been simulated using two sets of tooth stiffness factors. In the first case, a gradual change in factor α, from 1.0 to 0.70 in steps of 0.02, is used to simulate the gradual weakening of the tooth with a uniform rate of increase in the crack size. In the second case, α has been assumed to vary gradually at the initial stage from 1.0 to 0.98 in steps of 0.002 to simulate the slow crack initiation, then abruptly to 0.90 and finally to 0.70. The second case has been considered to simulate the abrupt change in tooth stiffness due to rapid weakening of the tooth before its failure.

Table 1: Gear model parameters

Parameter	Value
I_e	0.25 lb.s^2/in
s	1×10^6 lb/in
c	50 lb.s/in
F_e	1×10^3 lb
e_{mean}	1×10^{-6} in
$e_{\text{std deviation}}$	$1/3 \times 10^{-6}$ in

Equation (15) has been integrated using fourth-order Runge-Kutta method with a step size of 0.15 ms giving 500 data points for each rotation of the gears. Figure 1(a) shows the simulated steady state response of the gear vibration with no tooth crack. The random nature of the time response is due to the assumed normal distribution of the static transmission error. In Fig. 1(b), the time response is shown for $\alpha=0.99$. The effect of tooth weakening (1%) is evident in the periodic response. The time period of 0.075s, between two successive peaks, corresponds to the gear rotational speed. Figure 1(c) shows the response for $\alpha=0.70$. As expected the periodic response becomes even more prominent with a higher level of vibration amplitude.

The simulated gear signals have been processed further to extract the features, namely, SampEn, kurtosis, EI and PSEn for each level of the gear tooth crack. Figures 2(a)-(d) show the features for the second case of slow crack initiation followed with an abrupt change in tooth stiffness. In Fig. 2(a), SampEn starts with a high value corresponding to the random nature of the gear vibration without any tooth crack for the normally distributed transmission error. SampEn decreases as the gear response becomes more regular with the development of the tooth crack. The signal kurtosis in Fig. 2(b) starts with a value close to 3 implying the normal distribution of the gear response without crack and then increases with the weakening of the tooth. In Fig. 2(c), EI remains quite low during the initial stages of the crack and then increases due to higher amplitudes of gear vibration with weakening of the tooth. PSEn starts with a small value, remains small during the gradual change in tooth stiffness and jumps to higher value towards the end, see Fig. 2(d). It should be noted that all features except SampEn show higher values with reduction in tooth stiffness. To keep all the features positive during the crack development, difference of SampEn from its initial value, dSampEn(k)=SampEn(1)-SampEn(k), is used for all subsequent analysis. For the first simulated case of gradual tooth weakening, the extracted features follow similar trends, though more gradual. These plots are omitted for brevity.

HI based on the evolving averages of the features have been next obtained using the procedure discussed in earlier sections. Figure 3(a) shows the variations of the normalized HI with a gradual increase of the tooth crack size (represented as reduced tooth stiffness). The evolving average of kurtosis has also been computed and presented in Fig. 3(a) for comparison with other HI. EI and dSampEn (differential SampEn) have the highest sensitivity at the initial stage. Kurtosis and dSampEn show similar trends in the mid stage of the crack development and increase slowly towards the end. PSEn shows almost no change at the initial stage, then increases slowly till $\alpha\leq 0.98$ and finally rises sharply showing a high sensitivity.

Figure 3(b) shows similar trends except for the slightly higher slopes for HI based on EI and kurtosis near the region of abrupt change in tooth stiffness compared to the case of gradual change in Fig. 3(a).

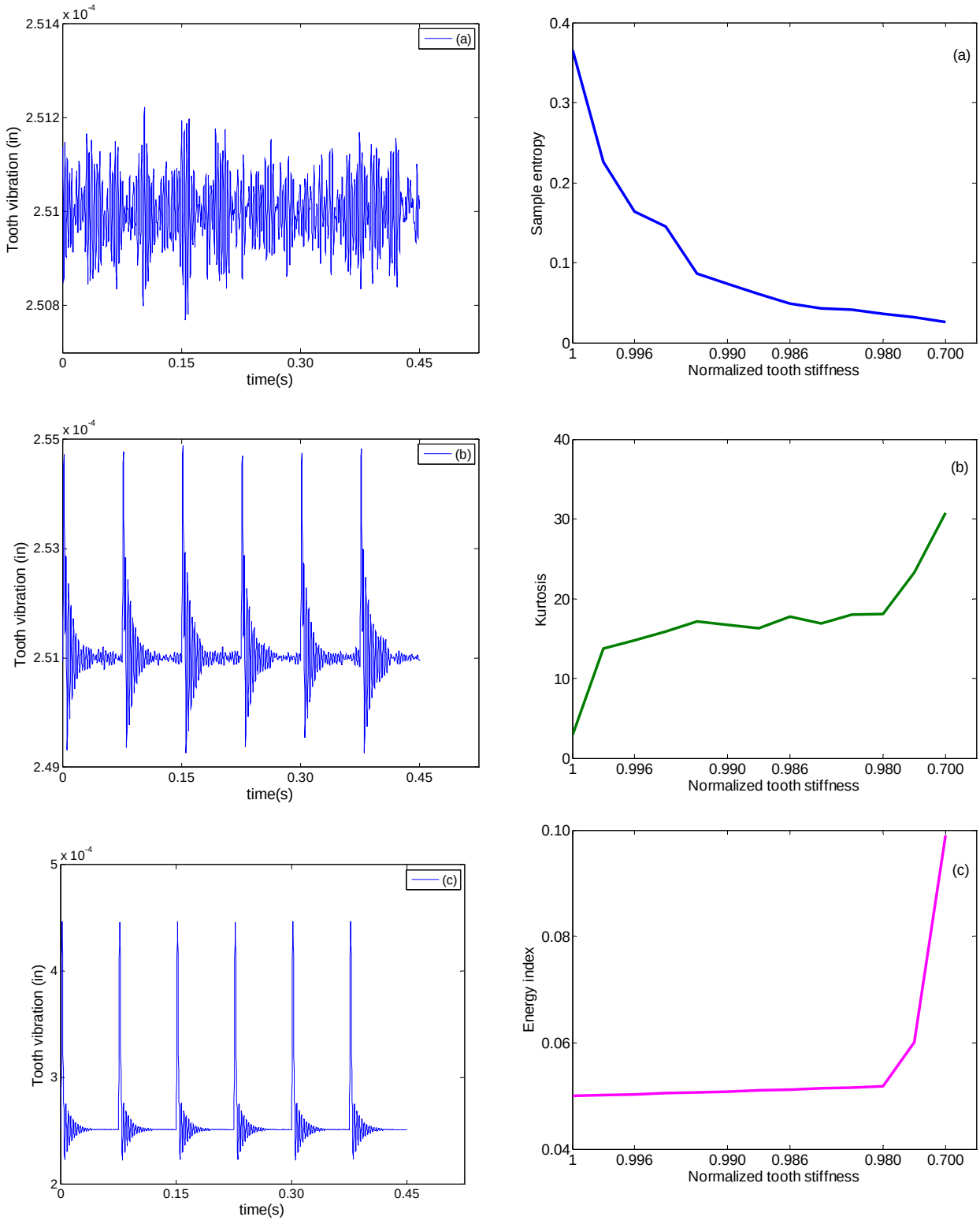

Figure 1: Simulated gear vibration for different levels of tooth fault, S=αs, (a) α=1, (b) α=0.99, (c) α=0.70.

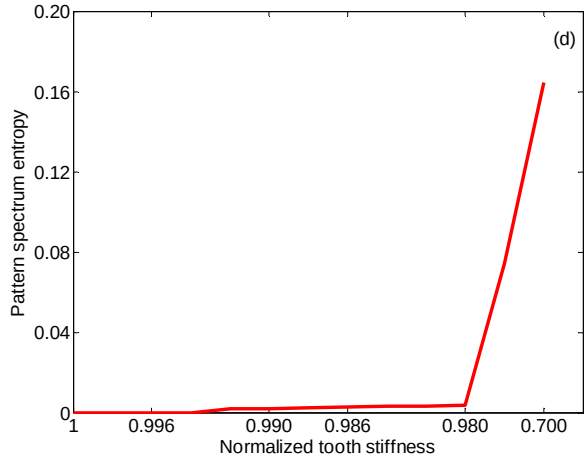

Figure 2: Features extracted from simulated gear vibration data (a) Sample entropy, (b) kurtosis, (c) Energy index, (d) Pattern spectrum entropy

It should be noted that the x-axes in Figs. 2(a)-(d) and Fig. 3(b) show two zones: gradual change from 1 to 0.980 and abrupt change from 0.980 to 0.700 corresponding to the simulation of case 2. The plots are helpful to compare qualitatively the relative changes in features in the two zones simulating, to some extent, the gear tooth crack.

7.2 HI for Vibration Data of Helicopter Gearbox

This section briefly presents the steps of extracting HI from the seeded gear fault vibration data of a helicopter drivetrain gearbox. Tests were conducted, from crack initiation to failure, on an intermediate gearbox pinion of a helicopter drivetrain with a small electric discharge notch at the root of a gear tooth (Hardman et al., 1999). The number of teeth on the input gear (pinion) and the output gear were 25 and 31 respectively with a tooth meshing frequency of 1.7145 kHz (corresponding to the input shaft speed of 4116 rpm). Two piezoelectric accelerometers were placed on the gearbox casing, one each at the input and the output side. The shaft speed data were recorded using a tachometer. Fourteen sets of data from the input side accelerometer were used for the present study covering the experimentation period. Time synchronous average (TSA) of 20 cycles over a complete revolution of the pinion for each time (corresponding to a level of gear tooth fault) has been used. The frequency spectrum of the average signals showed the presence of low frequency interference corresponding to the third harmonic of the gear meshing frequency. The signals have been high-pass filtered to eliminate this interference.

Each residual signal has been processed further to extract dSampEn, kurtosis and EI and the corresponding evolutionary averages for each level of the gear tooth fault.

The residual signals over one complete revolution of the pinion have been shifted to non-negative values by adding 1 for MSP. Each non-negative (shifted) signal has been subsequently processed through MSP to extract PS using a flat SE $=\{1\}_{10}$ with a size of 10 sample points (each having a value of 1). The width of basic SE has been selected based on the examination of the residual signal peaks and valleys. For multiscale MM and extraction of PS, the scales (n) upto 50 have been used. Each PS is further processed to extract PS entropy. The evolutionary averages of PS entropy have been obtained over the period of experiment.

Figure 4 shows the variations of normalized evolutionary averages of HI over the period of experimentation from the crack initiation to the failure of the gear tooth. All four indices show excellent sensitivity to the initiation of the gear tooth fault. The trends of EI and kurtosis based HI are similar though during the intermediate period of fault development, EI gives relatively higher values than the latter. Kurtosis based HI shows better sensitivity than EI near the total failure of the tooth. Both EI and kurtosis based HI keep fluctuating during the intermediate section. The curve of HI based on dSampEn drops to lower value towards the end and remains almost flat reducing its sensitivity to changes in gear tooth condition. This lack of sensitivity of SampEn based HI may be attributed to the lower values of SampEn with higher regularity of the gear signal. However, this issue needs further study.

The near flatness of the PSEn based HI curve in the intermediate section implies sustained level of the residual signal in the presence of fault. It implies that shape-size complexity measure (PSEn) remains less sensitive to the changes in signal amplitude in the intermediate stage of fault development. In other words, the signal shape remains relatively unchanged during the intermediate stage of tooth fault development. The steep slope of PSEn based HI towards the end of the experimentation period signifies almost complete failure of the gear tooth. PSEn and kurtosis based HI give better sensitivity to the imminent gear failure than other EI. The more regular shape of PSEn based index makes it a better candidate than others as a potential HI for machinery diagnostics and prognostics.

The proposed HI based on PSEn conforms to the expected ‘bathtub’ trend for fault status in engineering systems (Heng et al., 2009; Vachtsevanos et al., 2006). It is worth mentioning that the HI curves in Fig. 4 have been obtained using the dataset of an accelerated failure test of a gearbox. In actual cases, similar curves can be obtained with a much longer time span. These HI curves may be established from the legacy data of similar systems. A typical HI curve can be used for

detection and prognostics of the fault with user defined thresholds for each zone. For example, in the present case, the following may be used: fault detection level HI=0.5 and failure: HI>0.7.

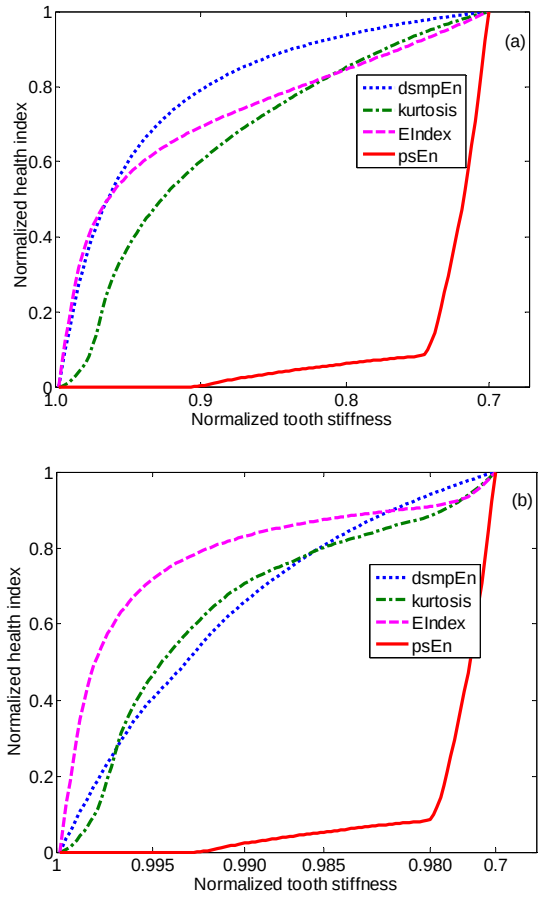

Figure 3: Normalized HI for simulated gear vibration data with increasing crack size (a) gradual change, (b) abrupt change

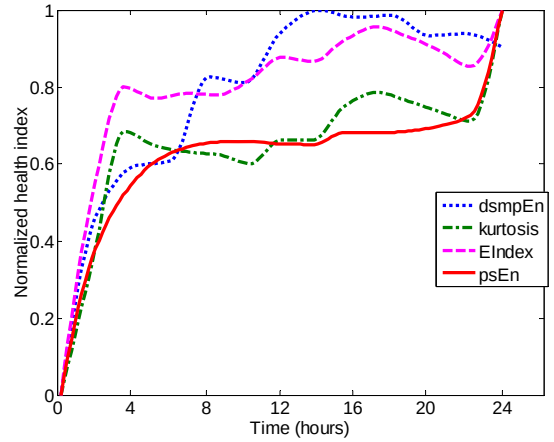

Figure 4: Normalized HI for helicopter gearbox vibration data

8 CONCLUSION

Health indices have been presented for machine condition monitoring and prognostics using morphology and complexity measures of vibration signals. The procedure has been illustrated using simulated gear vibration data and experimental dataset of a helicopter drivetrain gearbox. The features based on shape-size complexity (morphology) and information complexity measures have also been compared with an energy based feature and the commonly used signal kurtosis. All features give excellent sensitivity to the fault initiation for both simulated and experimental datasets. However, morphology based HI (PSEn) shows better sensitivity to the imminent failure than other features for the simulated dataset. For the experimental dataset, HI based on signal morphology shows the expected 'bathtub' trend of fault status. Though the features based on energy and kurtosis show progression with the crack, these suffer from fluctuations in the intermediate section of the failure period. The MSP based HI shows better characteristics than others as a viable HI. It would be interesting to apply the HI development process using more extensive datasets of in-service helicopter drive train gearboxes or similar systems in future. The extension of the technique to other types of rotating machinery will also be the subject of further study.

ACKNOWLEDGMENT

The helicopter gearbox data were acquired and provided by Naval Air Warfare Center Aircraft Division Helicopter Integrated Diagnostic System (HIDS) program at the Helicopter Transmission Test Facility (HTTF) Patuxent River, MD, USA. The work was carried out with partial support from Naval Sea Systems Command (NAVSEA) grant N00024-07-C-4212. This support is gratefully acknowledged (monitors: Marc Steinberg, R. Wagner and John Metzer).

REFERENCES

(Al-Balushi and Samanta, 2002) K. R. Al-Balushi and B. Samanta. Gear fault diagnosis using energy-based features of acoustic emission signals, *Proceedings of IMechE, Part I: Journal of Systems and Control Engineering*, vol. 216, pp. 249-263, 2002.

(Choi and Li, 2006) S. Choi and C. J. Li X. Estimation of gear tooth transverse crack size from vibration fusing selected gear condition indices, *Measurement Science and Technology*, vol. 17, pp. 2395-2400, 2006.

(Costa et al., 2005) M. Costa, A. L. Goldberger, and C. K. Peng. Multiscale entropy analysis of biological

signals, *Physics Review,* vol.71, paper id:021906, 2005.

(Hardman et al., 1999) W. Hardman, A. Hess, and J. Sheaffer. SH-60 helicopter integrated diagnostic system (HIDS) program- diagnostic and prognostic development experience, in *Proceedings of IEEE Aerospace Conference*, Aspen, CO, USA, March 6-13, pp. 473-491, 1999.

(He and Bechhoefer, 2008) D. He and E. Bechhoefer. Development and validation of bearing diagnostic and prognostic tools using HUMS condition indicators, in *Proceedings of 2008 IEEE Aerospace Conference*, Big Sky, MT, 2008.

(Heng et al., 2009) A. Heng, S. Zhang, A. C. C. Tan, and J. Mathew. Rotating machinery prognostics: state of the art, challenges and opportunities, *Mechanical Systems and Signal processing*, vol. 23, pp.724-739, 2009.

(Henry et al., 2002) B. Henry, N. Lovell, and F. Camacho. Nonlinear dynamics time series analysis. In *Nonlinear Biomedical Signal Processing, Vol. 2, Dynamic Analysis and Modeling*, Metin Akay (Ed.), ISBN: 9780780360129, 2002.

(Hochmann and Bechhoefer, 2003) D. Hochmann and E. Bechhoefer. Gear tooth crack signals and their detection via the FM4 measure in application for a helicopter HUMS (health usage and management systems), in *Proceedings of 2003 IEEE Aerospace Conference*, Big Sky, MT, pp. 3313-3326, 2003.

(Janjarasjitt et al., 2008) S. Janjarasjitt, H. Oack and K. A. Loparo. Bearing condition diagnosis and prognosis using applied nonlinear dynamical analysis of machine vibration signal, *Journal of Sound and Vibration*, vol. 317, pp. 112-126, 2008.

(Jardine et al., 2006) A. K. S. Jardine, D. Lin, and D. Banjevic. A review on machinery diagnostics and prognostics implementing condition-based maintenance, *Mechanical Systems and Signal Processing*, vol. 20, pp.1483-1510, 2006.

(Jia et al., 2006) W. Jia, R. J. Sclabassi, L.-S. Pon, M. L. Scheuer, and M. Sun. Spkie separation from EEG/EMG data using morphological filter and wavelet transform. Proceedings of 28th IEEE EMBS Annual International Conference, New York, NY, pp. 6137-6140, 2006.

(Li et al., 2008) X. Li, G. Ouyang and Z. Liang. Complexity measure of motor current signals for tool flute breakage detection in end milling, *International Journal of Machine Tools and Manufacture*, vol. 48, pp. 371-379, 2008.

(Maragos and Scafer, 1987) P. Maragos and R. Schafer. Morphological filters-part I: their set-theoretic analysis and relations to linear shift-invariant filters, *IEEE Transactions on Acoustics, Speech, and Signal Processing*, vol. 35, pp.1153- 1169, 1987.

(Maragos, 1989a) P. Maragos. A representation theory for morphological image and signal processing, *IEEE Transactions on Pattern Analysis and Machine Intelligence*, vol. 11, pp. 586-599, 1989.

(Maragos, 1989b) P. Maragos. Pattern spectrum and multiscale shape representation, *IEEE Transactions on Pattern Analysis and Machine Intelligence*, vol. 11, pp. 701-716, 1989.

(Nikolaou and Antoniadis, 2003) N. G. Nikolaou and I. A. Antoniadis. Application of morphological operators as envelope extractors for impulsive-type periodic signals, *Mechanical Systems and Signal Processing*, vol. 17, pp. 1147-1162, 2003.

(Pincus, 1991) S. M. Pincus. Approximate entropy as a measure of system complexity, *Proc Natl Acad Sci USA*, vol.88, pp. 2297-2301, 1991.

(Richman and Moorman, 2000) J. S. Richman and J.R. Moorman. Physiological time-series analysis using approximate entropy and sample entropy. *Am J Physiol Heart Circ Physiol* vol.278, pp.2039-2049, 2000.

(Samanta, 2004) Samanta, B. Gear fault detection using artificial neural networks and support vector machines with genetic algorithms. *Mechanical Systems and Signal Processing*, vol. 18, pp. 625-644, 2004.

(Samanta and Nataraj, 2008a) B. Samanta and C. Nataraj. Prognostics of machine condition using soft computing, *Robotics and Computer-Integrated Manufacturing*, vol. 24, pp. 816-823, 2008.

(Samanta and Nataraj, 2008b) B. Samanta and C. Nataraj. Prognostics using morphological signal processing and computational intelligence, in *Proceedings of 1st IEEE intl. Conf. PHM2008*, Denver, CO, 2008.

(Samanta and Nataraj, 2009a) B. Samanta and C. Nataraj. Use of particle swarm optimization for machinery fault detection. *Engineering Applications of Artificial Intelligence*, vol. 22, pp. 308-316, 2009.

(Samanta and Nataraj, 2009b) B. Samanta and C. Nataraj. Prognostics of machine condition using energy based monitoring index and computational intelligence, *Transactions of ASME*, *Journal of Computing and Information Science in Engineering, paper# JCISE 2008-55 (in press)*, 2009.

(Smith, 2003) J. D. Smith.. *Gear Vibration and Noise*, 2nd Edn., Mercel Dekker, New York, 2003.

(Sun et al., 2003) P. Sun, Q. H. Wu and A. M. Weindling, A. Finkelstein, and K. Ibrahim. An improved morphological approach to background normalization of ECG signals, *IEEE Transactions on Biomedical Engineering*, vol. 50, pp. 117-121,

2003.

(Sun et al., 2005) Y. Sun, K. L. Chan and S. M. Krishnan. Characteristic wave detection in ECG signal using morphological transform, *BMC Cardiovascular Disorders*, vol. 5, pp. 28-34, 2005.

(Vachtsevanos *et al., 2006*) G. Vachtsevanos, F. L. Lewis, M. Roemer, A. Hess, and B. Wu. *Intelligent Fault Diagnosis and Prognosis for Engineering Systems*, 1st ed. Hoboken, New Jersey: John Wiley & Sons, Inc, 2006.

(Wang et al., 2004) W. Wang, F. Ismail, and F. Golnaraghi. A neuro-fuzzy approach to gear system monitoring, *IEEE transactions on Fuzzy Systems*, vol. 12, pp. 710-723, 2004.

(Wang et al., 2009) J. Wang, G. Xu, Q. Zhang, and L. Liang. Application of improved morphological filter to the extraction of impulsive attenuation signals, *Mechanical Systems and Signal Processing*, vol. 23, pp. 236-245, 2009.

(Xu et al., 2007) G. Xu, J. Wang, Q. Zhang, S. Zhang, and J. Zhu. A spike detection method in EEG based on improved morphological filter, *Computers in Biology and Medicine*, vol. 37, pp. 1647-1652, 2007.

(Yan and Gao, 2007) R. Yan and R. X. Gao. Approximate entropy as a diagnostic tool for machine health monitoring, *Mechanical Systems and Signal processing*, vol. 21, pp. 824-839, 2007.

(Yu et al., 2006) Y. Yu, Y. Dejie, and C. Junsheng. A roller bearing fault diagnosis method based on EMD energy entropy and ANN, *Journal of Sound and Vibration*, vol. 294, pp. 269-277, 2006.

(Zakrajsek et al., 1995) J. Zakrajsek, D. Townshed, D. Lewicki, H. Decker, and R. Handschuh. Transmission diagnostic research at NASA Langley Research Center. *IMechE Conference Transactions, 2nd International Conference on Gearbox Noise, Vibration and Diagnostics*, London, UK, pp. 1-14, 1995.

(Zhang et al., 2008) L. Zhang, J. Xu, J. Yang, D. Yang, and D. Wang. Multiscale morphology analysis and its application to fault diagnosis, *Mechanical Systems and Signal Processing*, vol. 22, pp. 597-610, 2008.